Int. J. Electrochem. Sci., 17 **(2022)** Article Number: 220544, doi: 10.20964/2022.05.38

International Journal of
ELECTROCHEMICAL
SCIENCE
www.electrochemsci.org

Synthesis and Application of ZnO/Conductive Polymer Poly (3,4-ethylenedioxythiophene) (ZnO-PEDOT) Nanocomposite for Photodegrdation of Methyl Orange

BoAn Xiao

Zhengzhou Preschool Education College, Zhengzhou, 450000, China
E-mail: mjmj0815123@sina.com

Received: 11 January 2022 / *Accepted:* 8 March 2022 / *Published:* 5 April 2022

The chemical oxidative polymerization process was used to synthesize ZnO and the conductive polymer Poly (3,4-ethylenedioxythiophene) (ZnO-PEDOT) nanocomposite, which was then used to photodegrade methyl orange (MO). The results of morphology and crystallinity investigations suggested that ZnO spherical-shaped nanoparticles and shale-like PEDOT particles were successfully incorporated into the ZnO-PEDOT nanocomposite. The optical band gap values of PEDOT, ZnO, and ZnO-PEDOT nanocomposite were 1.80 eV, 3.43 eV, and 3.15 eV, respectively, according to UV-vis absorption analysis, and the narrow band gap of ZnO-PEDOT nanocomposite indicated to boost the efficiency for visible light harvesting. According to the EIS analysis, the ZnO-PEDOT has a lower charge-transfer resistance value than PEDOT and ZnO, indicating that the ZnO-PEDOT has higher catalytic activity due to the synergistic impact of ZnO and PEDOT. According to photocatalytic experiments, complete decolorization of 100, 50, 20, and 10 mg/l MO solutions was achieved after 120, 90, 80, and 70 minutes, respectively. Because of the simple synthesis method, superb adsorption capacity, good photocatalytic stability, and reproducibility of PEDOT, a comparison of the photocatalytic decolorization activity of ZnO-PEDOT nanocomposite with that of other reported literature for MO dye degradation revealed that the ZnO-PEDOT nanocomposite indicated effective performance for the decolorization of MO dye.

Keywords: PEDOT; ZnO; Nanocomposite; Methyl orange; Visible light harvesting; Photodegradation

1. INTRODUCTION

As a pH indicator, the anionic water-soluble azo dye methyl orange (MO, sodium; 4-[[4-(dimethylamino)phenyl]diazenyl]benzenesulfonate) is frequently used. It is widely employed in dye-requiring industries such as textiles, paint, paper, chemicals, printing, cosmetics, pharmaceuticals, and food industries, as well as research facilities, and local dye wastewater can be discharged into the environment, causing a variety of environmental issues [1, 2]. MO, Irritation of the respiratory tract

and effects on the central nervous system are possible side effects [3, 4]. It can also be carcinogenic because of its cleavage products, such as benzidine, which causes cancers in humans and animals [5-7].

Therefore, treatment of the dye contaminated wastewater is important before discharge into the environment [8, 9]. Adsorption, oxidation, ion exchange, ozonation, flocculation-coagulation, membrane filtration, catalytic and photocatalytic degradation, and biological and electrochemical treatment are the available techniques to treat dye-contaminated wastewater [10, 11]. Among them, photocatalytic degradation is a low-cost, non-toxic technique, and an effective way to deal with organic pollutants in wastewater, especially MO which is recalcitrant in nature and hard to degrade by conventional methods [12-14].

TiO_2 and ZnO are the widely used photocatalysts in dye degradation upon UV and visible light irradiation. The photogenerated electrons and holes can enhance the formation of active species which degrade the dye molecules [15-17]. However, the high recombination rate of photogenerated carriers and photoactivity in the UV region are the common problems in photocatalysts, and to overcome these problems, doping, hybrids and composites based on TiO_2 and ZnO can decrease the recombination rate and narrow the band gap to enhance the photocatalytic performance in the visible region [18-20]. Therefore, this study was conducted on synthesis and application of ZnO-PEDOT nanocomposite for photodegradation of methyl orange.

2. EXPERIMENTAL

2.1. Synthesis of ZnO-PEDOT nanocomposite

The ZnO-PEDOT nanocomposite was made using a chemical oxidative polymerization technique [21]. The oxidant and conductive polymer utilized were ammonium persulfate (APS, 99%, Merck, Germany) and PEDOT (97%, Sigma-Aldrich). 2g of ZnO nanopowder (>99%, 100 nm particle size, Sigma-Aldrich) was disseminated in 0.06M of EDOT monomer, and 4g of APS was added to the suspension. To finish the polymerization reaction, the mixture was agitated for 25 minutes and then kept at room temperature for 24 hours under flowing N2. The product was centrifuged at 1000 rpm, washed four times with a mixture of water and ethanol to remove any residual APS, and then dried under vacuum for 24 hours at 55°C.

2.2. Study of photocatalytic performance

The photocatalytic performance of ZnO and ZnO-PEDOT nanocomposite for MO dye degradation was investigated using a quartz tube placed around a visible light source (500 W tungsten lamp, Zhejiang Bozhou Marine Electric Technology Co., Ltd., China). 50 mL of MO solution was mixed with 5 mg of catalysts. Prior to light irradiation, the suspensions were magnetically stirred in the dark for 60 minutes to achieve desorption–adsorption equilibrium. Next, the mixture was irradiated by light sources and during irradiation, the mixture was stirred at a constant speed. The concentrations of

the MO solution were analyzed at the maximum absorption wavelength of the dye by a spectrophotometer (Milton Roy Spectronic 3000 Array, New York, USA). The decolorization efficiencies (η) of the MO are calculated by the following equation [22-24]:

$$\eta(\%) = \frac{C_0 - C_t}{C_0} \times 100 = \frac{I_0 - I_t}{I_0} \times 100 \qquad (1)$$

where C_0 and C represent the MO concentration before and after illumination (t), respectively. I_0 and I also represent the corresponding initial and degraded MO solution absorbance, respectively.

2.3. Characterization

The structural, morphological and optical properties of the prepared ZnO and ZnO-PEDOT nanocomposite were measured by X-ray diffraction (XRD diffractometer Shimadzu XRD-6000, Japan), Scanning electron microscopy (SEM) and UV–visible spectrophotometer (HR4000, Ocean Optics Inc., USA), respectively. Electrochemical impedance spectroscopy (EIS) measurements were conducted on an electrochemical work station (CHI6273D, CH Instruments, Inc., Austin, TX, USA) at frequency range from 10^{-2} Hz to 10^{5} Hz with an AC amplitude of 5 mV using an electrochemical cell consisting of PEDOT, ZnO and ZnO-PEDOT nanocomposite modified GCE as the working electrode, a saturated Ag/AgCl electrode as a reference and a Pt wire as counter electrode in 0.5 M Na_2SO_4 (99%, Shanghai Liangren Chemical Co., Ltd., China) solution. EIS Equivalent Circuit was modeled using ZSimpWin Software.

3. RESULTS AND DISCUSSION

3.1. Morphology and crystallinity analyses

SEM images of ZnO and ZnO-PEDOT nanocomposite are shown in Figure 1. The pure ZnO nanoparticles in the SEM image are spherical-shaped nanoparticles with an average diameter of 60 nm. Figure 1b shows that shale-like PEDOT particles are equally spread over ZnO nanoparticles, with an average diameter of 70 nm for ZnO-PEDOT particles.

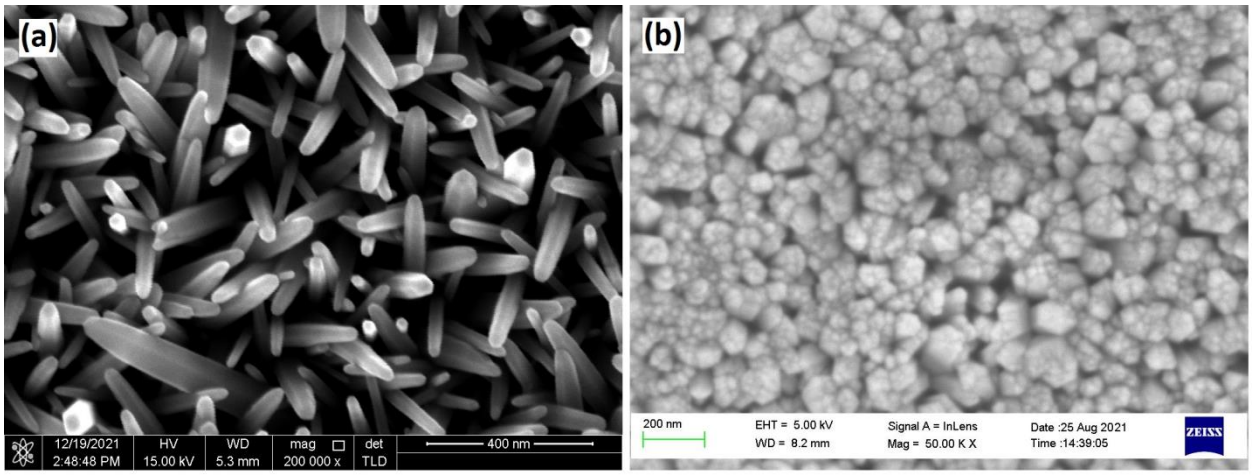

Figure 1. SEM images of (a) ZnO and (b) ZnO-PEDOT nanocomposite.

In Figure 2, the XRD patterns of PEDOT, ZnO and ZnO-PEDOT nanocomposite are preseted. As seen in Figure 2a, the pure PEDOT shows only one broad diffraction peak with low intensity at 25.81°, which can be attributed to intermolecular π→π* stacking of polymer backbone related to the (020) reflection [25]. XRD patterns of ZnO and ZnO-PEDOT nanocomposite display the diffraction peaks at 31.39°,34.09°, 35.89°, 47.29°, 56.36°, 62.71, 67.81°, 72.49°,and 76.72°, which are correspond to the (100), (002), (101), (102), (110), (103), (112), (004) and (202) crystal planes of the hexagonal wurtzite ZnO, respectively (JCPDS card No. 36-1451) [26]. The XRD pattern of the ZnO-PEDOT nanocomposite shows the additional peak of (020) PEDOT that indicate successful incorporations of ZnO and PEDOT into the ZnO-PEDOT nanocomposite.

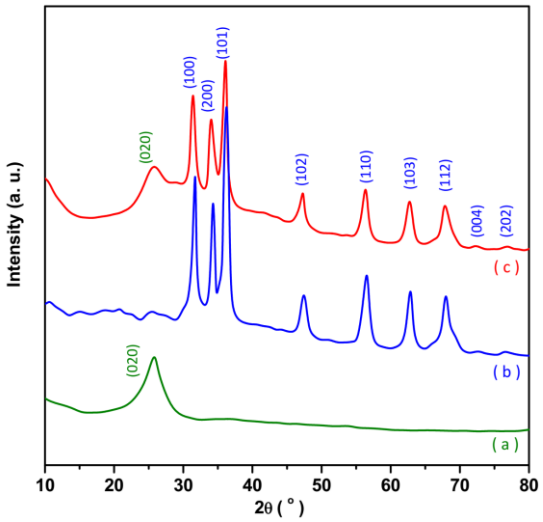

Figure 2. XRD patterns of (a) PEDOT, (b) ZnO and (c) ZnO-PEDOT nanocomposite.

3.2. UV-vis absorption spectra

The UV-vis absorption spectra of PEDOT, ZnO, and ZnO-PEDOT nanocomposite are shown in Figure 3a. According to numerous studies, the optical band gap values of ZnO and PEDOT are in the range of 3.1-3.55 eV for ZnO and 1.6-2.18 eV for PEDOT [27-29]. As can be seen in Figure 3a, ZnO can only absorb light in the UV area, with its absorption edge at 390 nm. Because a photon with sufficient energy may excite electrons from its filled valence band and empty conduction band in the ground state, ZnO works as a good photosensitizer in the UV area for photocatalytic activities [30-32]. However, the sensitization process on ZnO is always dominated by the relative position of the conduction band of the wide bandgap ZnO which limits absorption only within the UV region and also by the nature of the interfaces in the system which accelerates recombination of photogenerated electron–hole pairs [33]. Furthermore, previous reports have indicated that doping of ZnO or adding the metrials in ZnO based nanocoposites can change the optical band gap value due to chang in crystal stucture, grain size, conductivity and formation of an intermediate band [34, 35].

Furthermore, Figure 3a also shows that PEDOT reveals strong absorption in both of UV and

visible light regions, it's related to the onset of the π-π* absorption in PEDOT [21]. In addtition, the electronic band gap of the PEDOT chain can be controlled by the bonding and antibonding of steric interactions along the chain backbone [36, 37]. UV-via absorption spectra for ZnO-PEDOT nanocomposite reveal improved absorption in UV and visible light regions toward ZnO, which promotes the performance of ZnO-PEDOT nanocomposite across the full UV-vis spectrum. It has been linked to an increase in nanocomposite conductivity [38], and attributed to the creation of impurity levels in the bandgap of ZnO which decreases the carrier concentration donated by interstitial zinc atoms or oxygen vacancies and causes the Fermi level to shift to lower energies, and as consequence, decreases the optical band gap value of ZnO-PEDOT nanocomposite [39]. Figure 3b shows the results of calcultion the value of the optical band gap (E_g) by the Tauc's plot formula [40]:

$$(\alpha hv)^{1/2} = A(hv - E_g) \qquad (2)$$

Where α present's absorption coefficient, hν is incident photon energy, A is energy-independent constant, and Eg is the optical band gap. Therefore, the optical band gap values of PEDOT, ZnO and ZnO-PEDOT nanocomposite are 1.80 eV, 3.43 eV and 3.15 eV, respectively, which are determined by linear extrapolation from the photon energy (x) axis. The narrow band gap of ZnO-PEDOT nanocomposite results indicate a strong interaction between PEDOT and nano-ZnO [41]. Thus, the addition of the conductive polymer in the ZnO structure leads to a narrowing of the band gap and increases the efficiency of visible light harvesting [42, 43]. The narrow band gap may be related to the wrapping of conductive polymer on the ZnO surface [44]. Furthermore, the narrow band gap causes charge injection from the narrow band gap semiconductor to the wide band gap semiconductor, resulting in prolonged charge carrier separation by reducing photogenerated electron–hole pair recombination during photocatalysis [42].

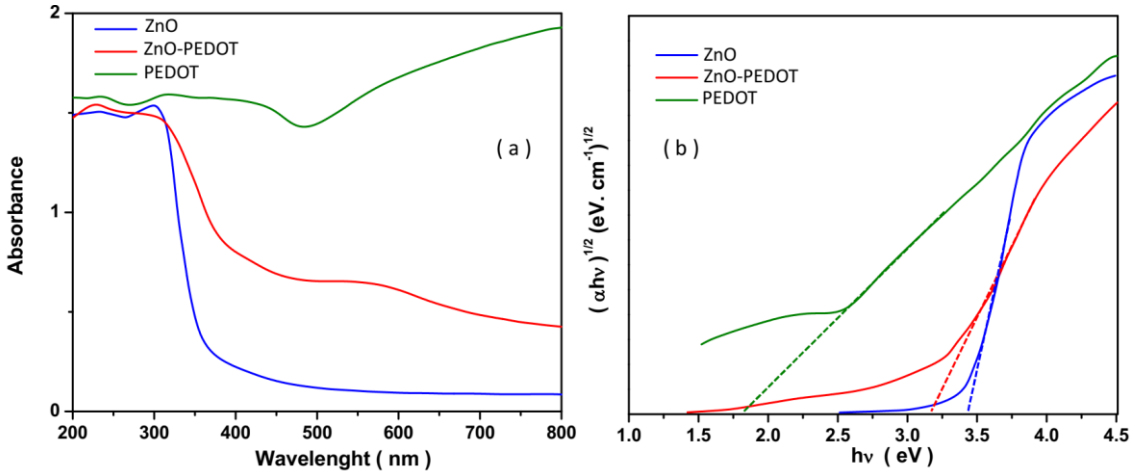

Figure 3. (a) UV-vis absorption spectra and (b) Tauc's plots of PEDOT, ZnO and ZnO-PEDOT nanocomposite.

3.2. Electrochemical impedance studies

The Nyquist plots and equivalent circuit model of PEDOT, ZnO, and ZnO-PEDOT nanocomposite modified GCE are shown in Figure 4. The radius of semicircles in the middle-

frequency band can be used to calculate the charge-transfer resistance (Rct) of each sample [45, 46]. The Rct of the PEDOT, ZnO, and ZnO-PEDOT nanocomposite modified GCE cells is 160.2, 599.4, and 98.9 Ω.cm^2, respectively. The ZnO-PEDOT has a lower Rct than PEDOT and ZnO, indicating that the ZnO-PEDOT has stronger catalytic activity due to the synergistic impact of ZnO and PEDOT.

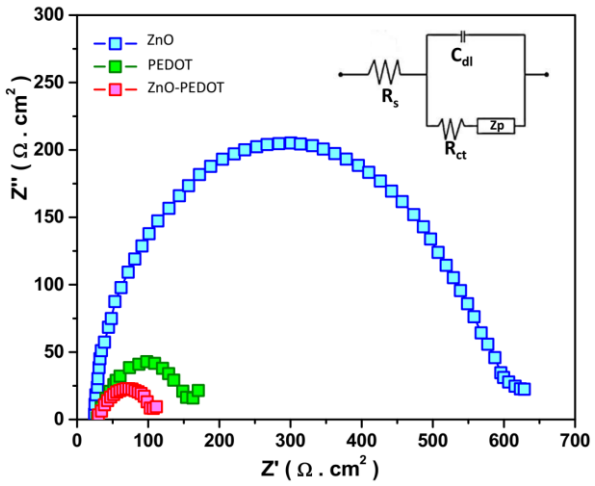

Figure 4. Nyquist plots and equivalent circuit model of PEDOT, ZnO and ZnO-PEDOT nanocomposite modified GCE.

3.4. Photocatalytic performance

Figure 5 shows the photocatalytic activity of ZnO, PEDOT, and ZnO-PEDOT nanocomposite as photocatalysts for the decolorization of 50 mL of 50 mg/l MO dye under visible light at various irradiation durations. The decolorization efficiency of the MO was tested in the dark and without photocatalysts for comparison, and the results demonstrate that the degradation of the MO after 60 minutes in the dark in the presence and absence of photocatalysts is negligible. The comparison of decolorization efficiency in the presence and absence of photocatalysts under visible light shows that there is no substantial degradation in the absence of photocatalysts and that photocatalysts play a major role in MO dye degradation.

As depicted in Figure 5, MO dye can be degraded by ZnO, PEDOT and ZnO-PEDOT nanocomposite upon visible light irradiation, and the decolorization efficiency after 60 minutes visible light irradiation is 42%, 70% and 80% for ZnO, PEDOT and ZnO-PEDOT nanocomposite, respectively, and the complete decolorization is achieved after 125, 110 and 90 minutes, respectively. The higher decolorization efficiency of the ZnO-PEDOT nanocomposite comes from the synergistic effect between ZnO and PEDOT. PEDOT based photocatalyst shows good recyclability and great stability in the presence of oxidative species, such as superoxide anion radicals, $O_2^{\cdot -}$, hydroxyl radicals [47-49]. Moreover, PEDOT as an excellent hole conducting material can improve the hole transfer from ZnO to PEDOT [47, 50]. The optical band gap of ZnO-PEDOT nanocomposite shows a demonstrative decrease compared to ZnO, which develops the decolorization efficiency upon visible

light illumination [51, 52]. Besides, in the ZnO-PEDOT nanocomposite, some of the photogenerated electrons in the conduction band of ZnO can be transferred to the position of the highest occupied molecular orbital of the PEDOT [53]. The rate of these electrons can be faster than the rate of recombination of the photogenerated electrons and holes between the valence band and conduction band of the ZnO because of the proximity of the highest occupied molecular orbital position in the PEDOT to the conduction band of the ZnO [47, 51].

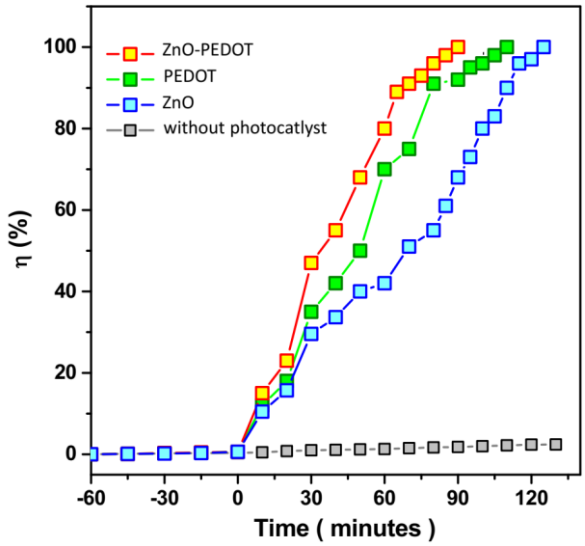

Figure 5. The results of photocatalytic activity of ZnO, PEDOT and ZnO-PEDOT nanocomposite as photocatalyst to decolorization of 50 mL of 50 mg/l MO dye upon visible light source at different irradiation times

Figure 6 shows the photocatalytic decolorization activity of the ZnO-PEDOT nanocomposite for removing 50 mL of various concentrations of MO solution when exposed to visible light. It is shown that as the initial concentration of dye increases, the rate of degradation decreases, which is associated with a constant rate of generation of oxidative species in a fixed amount of photocatalyst during photodegradation, and as a result, the rate of photocatalytic degradation decreases. After 120, 90, 80, and 70 minutes, complete decolorization of 100, 50, 20, and 10 mg/l MO solutions is accomplished, accordingly [54].

The comparison between the photocatalytic decolorization activity of ZnO-PEDOT nanocomposite and other reported literature for MO degradation can be shown in Table 1. Because of the simple synthesis process and excellent adsorption capacity, photocatalytic stability, and reproducibility of PEDOT, the ZnO-PEDOT nanocomposite shows effective performance for the decolorization of MO dye [55].

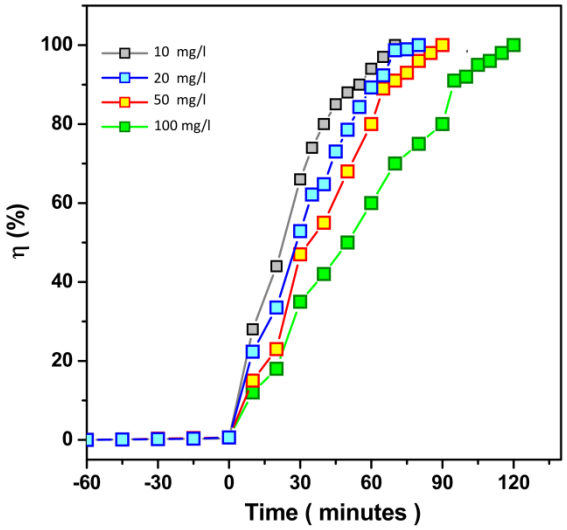

Figure 6. Photocatalytic decolorization activity of ZnO-PEDOT nanocomposite for remove of 50 mL of different concentrations of MO solution upon visible light irradiation.

Table 1. Comparison between the photocatalytic decolorization activity of ZnO-PEDOT nanocomposite and the other reported literature for degradation MO

Photocatalyst	MO concentration **(mg/l)**	**Light source**	**Degradation time (minute)**	**η(%)**	**Ref.**
ZnO/graphene oxide	10	UV	120	95	[18]
Fe_2O_3-TiO_2 composites	10	UV	25	87.8	[19]
ZnO nano-mushrooms	10	UV	210	92	[20]
ZnO–SiO_2	10	Visible	240	98	[56]
TiO_2/SiO_2/$NiFe_2O_4$	10	UV	300	90	[57]
ZnO nanoneedle	10	UV	140	95.4	[58]
Graphene/ZnO nanorods	15	UV-Visible	240	89	[59]
N-doped TiO_2	20	UV	100	98	[60]
Fe-doped TiO2 nanotubes	20	UV- visible	180	99.7	[61]
ZnO–SiO_2	50	Visible	240	55	[56]
ZnO-PEDOT	100	Visible	120	100	This work
	50		90		
	20		80		
	10		70		

4. CONCLUSION

This work was conducted on the synthesis of ZnO-PEDOT nanocomposite using a chemical oxidative polymerization method and its application for photodegradation of MO. Results indicated successful incorporations of ZnO and PEDOT nanoparticles into nanocomposites. An optical study revealed that the optical band gap values of PEDOT, ZnO and ZnO-PEDOT nanocomposite were 1.80

eV, 3.43 eV and 3.15 eV, respectively, and the narrow band gap of ZnO-PEDOT nanocomposite was indicated to increase the efficiency of visible light harvesting. The EIS study demonstrated a lower charge-transfer resistance value of the ZnO-PEDOT compared to PEDOT and ZnO. Photocatalytic studies showed that complete decolorization of 100, 50, 20 and 10 mg/l MO solutions was achieved after 120, 90, 80 and 70 minutes, respectively. The effective performance of the ZnO-PEDOT nanocomposite for the decolorization of MO is related to the synergistic effect of ZnO and PEDOT.

References

1. T. Zhang, X. Wu, S.M. Shaheen, H. Abdelrahman, E.F. Ali, N.S. Bolan, Y.S. Ok, G. Li, D.C. Tsang and J. Rinklebe, *Journal of hazardous materials*, 425 (2022) 127906.
2. D. Ge, H. Yuan, J. Xiao and N. Zhu, *Science of The Total Environment*, 679 (2019) 298.
3. H.K. Ebrahimi, S. Sohrabi, S. Jafarnejad, S. Iranmanesh and S. Esmaeilian, *Systematic Reviews in Pharmacy*, 11 (2020) 899.
4. H. Maleh, M. Alizadeh, F. Karimi, M. Baghayeri, L. Fu, J. Rouhi, C. Karaman, O. Karaman and R. Boukherroub, *Chemosphere*, (2021) 132928.
5. R.S. Bangari, A. Yadav and N. Sinha, *Soft Matter*, 17 (2021) 2640.
6. D. Ge, W. Wu, G. Li, Y. Wang, G. Li, Y. Dong, H. Yuan and N. Zhu, *Chemical Engineering Journal*, 437 (2022) 135306.
7. N.M. Mohamed, R. Bashiri, F.K. Chong, S. Sufian and S. Kakooei, *international journal of hydrogen energy*, 40 (2015) 14031.
8. W. Zhu, C. Hou, Q. Zhang and J. Liang, *Journal of Coastal Research*, 103 (2020) 835.
9. F. Husairi, J. Rouhi, K. Eswar, A. Zainurul, M. Rusop and S. Abdullah, *Applied Physics A*, 116 (2014) 2119.
10. F. Chen, J. Ma, Y. Zhu, X. Li, H. Yu and Y. Sun, *Journal of Hazardous Materials*, 426 (2022) 128064.
11. S. Khosravi and S.M.M. Dezfouli, *Systematic Reviews in Pharmacy*, 11 (2020) 913.
12. A. Ahmad, S.H. Mohd-Setapar, C.S. Chuong, A. Khatoon, W.A. Wani, R. Kumar and M. Rafatullah, *RSC advances*, 5 (2015) 30801.
13. W. Liu, J. Li, J. Zheng, Y. Song, Z. Shi, Z. Lin and L. Chai, *Environmental Science & Technology*, 54 (2020) 11971.
14. N. Naderi, M. Hashim, J. Rouhi and H. Mahmodi, *Materials science in semiconductor processing*, 16 (2013) 542.
15. J. He, P. Xu, R. Zhou, H. Li, H. Zu, J. Zhang, Y. Qin, X. Liu and F. Wang, *Advanced Electronic Materials*, (2021) 2100997.
16. M. Nazeer, F. Hussain, M.I. Khan, E.R. El-Zahar, Y.-M. Chu and M. Malik, *Applied Mathematics and Computation*, 420 (2022) 126868.
17. S. Khosravi, S.M.H. Sadati, V.A.S. Sherafat and Z. Bazargani, *Pakistan Journal of Medical & Health Sciences*, 14 (2020) 1753.
18. V.N. Nguyen, D.T. Tran, M.T. Nguyen, T.T.T. Le, M.N. Ha, M.V. Nguyen and T.D. Pham, *Research on Chemical Intermediates*, 44 (2018) 3081.
19. L. Wu, H. Yan, J. Xiao, X. Li, X. Wang and T. Zhao, *Ceramics International*, 43 (2017) 14334.
20. R. Kumar, G. Kumar and A. Umar, *Materials Letters*, 97 (2013) 100.
21. Z. Katančić, S. Šuka, K. Vrbat, A. Tašić and Z. Hrnjak-Murgić, *Chemical and Biochemical Engineering Quarterly*, 31 (2017)
22. K. Abe, *International Journal of Electrochemical Science*, 16 (2021) 21106.

23. D. Tan, H. Long, H. Zhou, Y. Deng, E. Liu, S. Wang and S. Zhang, *International Journal of Electrochemical Science*, 15 (2020) 12232.
24. Y.-M. Chu, B. Shankaralingappa, B. Gireesha, F. Alzahrani, M.I. Khan and S.U. Khan, *Applied Mathematics and Computation*, 419 (2022) 126883.
25. L. Zhang, R. Jamal, Q. Zhao, M. Wang and T. Abdiryim, *Nanoscale research letters*, 10 (2015) 1.
26. J. Rouhi, C.R. Ooi, S. Mahmud and M.R. Mahmood, *Materials Letters*, 147 (2015) 34.
27. A.H. Ismail, M.N. Mustafa, A.H. Abdullah, R.M. Zawawi and Y. Sulaiman, *Journal of The Electrochemical Society*, 163 (2015) G7.
28. G. Wang and Y. Hu, *Journal of Coastal Research*, 103 (2020) 956.
29. S. Vaziri, R. Mosaddegh, M. Rezai, F. Mohammadi and M.A. Ashari, *Journal of Critical Reviews*, 7 (2019) 2020.
30. M. Samadi, M. Zirak, A. Naseri, E. Khorashadizade and A.Z. Moshfegh, *Thin Solid Films*, 605 (2016) 2.
31. M. Mirzamoradi, M. Bakhtiyari, P. Kimiaee, A. Hosseini-Najarkolaei and M.A. Mansournia, *Archives of gynecology and obstetrics*, 292 (2015)
32. M. Husairi, J. Rouhi, K. Alvin, Z. Atikah, M. Rusop and S. Abdullah, *Semiconductor Science and Technology*, 29 (2014) 075015.
33. M.A. Johar, R.A. Afzal, A.A. Alazba and U. Manzoor, *Advances in Materials Science and Engineering*, 2015 (2015) 934587.
34. A. Srivastava, N. Kumar and S. Khare, *Opto-Electronics Review*, 22 (2014) 68.
35. X. Chen, D. Wang, T. Wang, Z. Yang, X. Zou, P. Wang, W. Luo, Q. Li, L. Liao and W. Hu, *ACS applied materials & interfaces*, 11 (2019) 33188.
36. E.-G. Kim and J.-L. Brédas, *Journal of the American Chemical Society*, 130 (2008) 16880.
37. T.H. Zhao, M.I. Khan and Y.M. Chu, *Mathematical Methods in the Applied Sciences*, (2021) 1.
38. A.O. Elbkosh, *Acta Electronica Malaysia*, 4 (2020) 35.
39. X.H. Nguyen, H.N. Luong, H.A. Pham, N.M. Nguyen and V.Q. Dang, *RSC Advances*, 11 (2021) 36340.
40. H.S. Abdulla and A.I. Abbo, *International Journal of Electrochemical Science*, 7 (2012) 10666.
41. T. Abdiryim, A. Ali, R. Jamal, Y. Osman and Y. Zhang, *Nanoscale research letters*, 9 (2014) 89.
42. S. Sardar and S.K. Pal, *Nanotechnology Reviews*, 5 (2016) 113.
43. M. Alimanesh, J. Rouhi and Z. Hassan, *Ceramics International*, 42 (2016) 5136.
44. M.B. Poudel, C. Yu and H.J. Kim, *Catalysts*, 10 (2020) 546.
45. L. Yuan, X. Qiu, L. Chen and W. Zhu, *Journal of Power Sources*, 189 (2009) 127.
46. J. Rouhi, S. Mahmud, S.D. Hutagalung, N. Naderi, S. Kakooei and M.J. Abdullah, *Semiconductor Science and Technology*, 27 (2012) 065001.
47. J. Liu, Danielle L. McCarthy, L. Tong, M.J. Cowan, J.M. Kinsley, L. Sonnenberg, K.H. Skorenko, S.M. Boyer, J.B. DeCoste, W.E. Bernier and W.E. Jones, *RSC Advances*, 6 (2016) 113884.
48. Q. Zhou, D. Liu, G. Yuan, Y. Tang, K. Cui, S. Jiang, Y. Xia and W. Xiong, *Separation and Purification Technology*, 281 (2022) 119735.
49. A. Bahrami, S. Jafarnejad, H. khoshnezhad Ebrahimi, S.M.M. Dezfouli and R. Pahlevani, *Systematic Reviews in Pharmacy*, 11 (2020) 905.
50. S.M.M. Dezfouli and S. Khosravi, *Pakistan Journal of Medical & Health Sciences*, 14 (2020) 1236.
51. F. Nur Indah Sari, M.-T. Syue, Y. Purba and J.-M. Ting, *Separation and Purification Technology*, 278 (2021) 119650.

52. Y.-M. Chu, U. Nazir, M. Sohail, M.M. Selim and J.-R. Lee, *Fractal and Fractional*, 5 (2021) 119.
53. A. Adam, *Acta Electronica Malaysia*, 4 (2020) 31.
54. P. Karimian and M.A. Delavar, *Pakistan Journal of Medical & Health Sciences*, 14 (2020) 1405.
55. Z. Lu, Z. Yu, J. Dong, M. Song, Y. Liu, X. Liu, Z. Ma, H. Su, Y. Yan and P. Huo, *Chemical Engineering Journal*, 337 (2018) 228.
56. H. He, S. Xue, Z. Wu, C. Yu, K. Yang, G. Peng, W. Zhou and D. Li, *Chinese Journal of Catalysis*, 37 (2016) 1841.
57. J. Kaur, S. Bansal and S. Singhal, *Physica B: Condensed Matter*, 416 (2013) 33.
58. N. Tripathy, R. Ahmad, J.E. Song, H.A. Ko, Y.-B. Hahn and G. Khang, *Materials Letters*, 136 (2014) 171.
59. M. Yu, Y. Ma, J. Liu, X. Li, S. Li and S. Liu, *Applied Surface Science*, 390 (2016)
60. F. Peng, L. Cai, L. Huang, H. Yu and H. Wang, *journal of Physics and Chemistry of Solids*, 69 (2008) 1657.
61. L. Deng, S. Wang, D. Liu, B. Zhu, W. Huang, S. Wu and S. Zhang, *Catalysis Letters*, 129 (2009) 513.